Int. J. Electrochem. Sci., 8 **(2013)** 6889 - 6899

International Journal of
ELECTROCHEMICAL
SCIENCE
www.electrochemsci.org

Electroless Plating Growth Au-Ag Core-Shell Nanoparticles for Surface Enhanced Raman Scattering

Tung-Hao Chang [1], *Yu-Cheng Chang* [2,3,*], *Fu-Hsiang Ko* [2], *Fu-Ken Liu*[3,*]

[1]Department of Radiation Oncology, Changhua Christian Hospital, Changhua, 50006, Taiwan,
[2]Department of Materials Science and Engineering, National Chiao Tung University, Hsinchu, 30010, Taiwan
[3]Department of Applied Chemistry, National University of Kaohsiung, Kaohsiung, 81148, Taiwan
[*]E-mail: ychang0127@gmail.com; fkliu@nuk.edu.tw

Received: 19 March 2013 / *Accepted:* 9 April 2013 / *Published:* 1 May 2013

Au core-Ag shell nanoparticles (NPs) have been grown on the silicon substrate with self-assembled well-define Au NPs by electroless plating method. The holding time of spin-coating strategy is a facile method for controlling the densities of Au NPs and treating them as an electrode for selective growth of Ag shell. The volumes of silver nitrate play an important role in growing the different shell thicknesses of Au-Ag core-shell NPs. The appropriate shell thicknesses and the densities of Au-Ag core-shell NPs were optimized to yield the greatest surface-enhanced Raman scattering (SERS) effect in rhodamine B molecule. The combination spin-coating strategy and electroless silver plating provide a facile and low cost fabrication method to prepare the different shell thicknesses and densities of Au-Ag core-shell NPs with high SERS enhancement, which shall be of significant value for practical applications of biosensor systems.

Keywords: Nanoparticles; Electroless; Self-assembly; Spin-coating; Surface-enhanced Raman Scattering

1. INTRODUCTION

Recently, bimetallic core-shell nanoparticles (NPs) have attracted extensive interest due to the addition of the second metal shell provides a method to control chemical or physical properties of the NPs [1-4]. Bimetal core-shell NPs are also an important class of nanostructures for both fundamental science and real applications such as in biomedical applications, magnetic, catalytic and optical properties [1-8]. Many kinds of core-shell NPs have been synthesized through various methods, such as electroless plating [9], surface precipitation reaction [10], surface reaction [11], seeding-mediated

[1], and self-assembly [8]. Electroless plating is a chemical reduction process which depends upon the catalytic reduction process of metal ions in an aqueous solution (containing a chemical reducing agent) and the subsequent deposition of metal without the use of electrical energy [12-14]. It can provide for a very efficient and facile method to control the shell thicknesses of NPs.

Gold (Au) and silver (Ag) NPs have received considerable attention for many years because of their fascinating optical properties known as localized surface plasmon resonance (LSPR), and their widespread use in applications related to photonics, catalysis, information storage, chemical/biological sensing, and surface-enhanced Raman scattering (SERS) [15]. SERS is a highly sensitive and selective technique that allows for detection of chemical or biological molecules in very low concentrations and provides rich structural information [16]. The ability to develop SERS substrates with strong enhancement factors, low cost, good stability and high reproducibility is still an important challenge [17]. The success of SERS is highly dependent on the interaction between adsorbed molecules and the surface of plasmonic nanostructures [18]. The size, morphology and composition of surface plasmon band should lead to control the intensity of SERS [19,20]. Comparison of the calculated and measured surface plasmon extinction spectra was repeatedly employed as one of the criteria of distinguishing between alloy and core-shell structure of the bimetallic Au-Ag NPs [21]. Up to now, a strategy for extracting optical constants of the Au-Ag core-shell NPs from their measured surface plasmon extinction spectra has been reported [22]. Furthermore, it was shown that Au-Ag core-shell NPs can be employed as SERS-active surfaces. SERS enhancement as a function of the core-shell Au-Ag NP composition and the state of their aggregation was investigated using pyridine and other types of probe adsorbates [23,24].

The present study has successfully synthesized the different shell thicknesses and uniform sizes of Au core-Ag shell NPs by electroless plating method. The appropriate volumes of silver nitrate are important for growing the different thicknesses of Ag shell in aqueous solution. The holding time of spin-coating strategy was exploited to control the densities of Au NPs on a 3-aminopropyltrimethoxysilane (APTMS)-modified silicon substrate and treating them as an electrode for selective growth of Ag shell. Both shell thicknesses and densities of Au-Ag core-shell NPs were optimized to yield the greatest SERS effect of rhodamine B molecule. The fabrication of Au NPs and Au-Ag core-shell NPs is easy, low cost, and high efficient, making it conducive to practical biosensor applications, and especially in nanoscale dimension.

2. EXPERIMENT

2.1 Materials and reagents

Trisodium citrate, hydrogen tetrachloroaurate(III) trihydride ($HAuCl_4$), silver nitrate($AgNO_3$), ascorbic acid and 3-aminopropyltrimethoxysilane (APTMS) were purchased from Acros. HPLC grade of ethanol was purchased from J. T. Baker. De-ionic water (>18 MΩ cm^{-1}) was used throughout the preparation of the Au NPs.

2.2 Preparation of Au NPs

Au-core NPs with 13 nm diameters were synthesized by adding 1 mL of 38.8 mM trisodium citrate to 10 mL aqueous solution of boiling 1 mM hydrogen tetrachloroaurate(III) trihydride under vigorous stirring. After appearance of a deep red color, boiling and stirring were continued under refluxing for 10 min and then cooled at room temperature. Si (100) wafer were cleaned in a boiling piranha solution (H_2O_2:concentrated H_2SO_4, 3:7, v/v) for 10 min, and then rinsed with de-ionized water and ethanol. The synthesis of Au NPs and their self-assembled on silicon substrate procedures were similar to our previous work [25, 26]. Briefly, the Au NPs were self-assembled on 1 cm × 1 cm Si (100) wafer that pre-fabricated with sandwich structure of Si wafer/thin oxide layer/organic amine terminal layer.

2.3 Preparation of Au-Ag core-shell NPs

Au-Ag core-shell NPs were grown by an electroless plating method in 25 mL of aqueous solution containing 10 mM ascorbic acid, and the different volumes of $AgNO_3$ solution (5 mM) was added dropwise. The substrate was positioned at the side of the beaker and under vigorous stirring. This electroless plating process was allowed to proceed for 30 min at room temperature, the substrate was immediately rinsed with de-ionized water and dried under a N_2 purge. The uniform morphology of Au-Ag core-shell NPs were grown by heating of the substrates at 400 °C for 1 hr in N_2 atmospheric.

2.4 Apparatus

The morphology of Au NPs and Au-Ag core-shell NPs on silicon substrate were monitored by a field emission scanning electron microscope (FESEM) using a JEOL JSM-6700F SEM operating at 10 kV accelerating voltage. A JEOL-2010 transmission electron microscope (TEM) operating at 200 kV was used to examine the microstructures. An electron dispersive spectrumeter (EDS) attached to the TEM was used to determine the composition of NPs. A Hitachi U-3310 UV-vis spectroscopy was employed to characterize the optical properties of NPs. The Raman spectra are performed by Confocal Raman Microscope (HOROBA, LabRAM HR) at room temperature in the backscattering configuration. The source light is He-Ne laser emitting at a wavelength of 632.8 nm.

3. RESULTS AND DISCUSSION

Figure 1a depicts the method used to self-assembly Au NPs. The fabrication processes can be briefly divided into two steps: (1) APTMS-functionalization of the Si substrate and (2) self-assembly of Au NPs on APTMS. The first step deposits a large-scale monolayer APTMS on the Si (100) wafer using a thin native oxide layer. The second step deposits the Au NPs onto the amino-terminated bonding using a spin-coating method. After dipping the substrate in a solution of Au NPs, holding for the desired time duration, and spinning out the extra solution using a spin coater at a speed of 1000

rpm, the substrate is immediately rinsed with de-ionized water and dried under a N_2 purge. Figure 1b depicts the method used to fabricate Au-Ag core-shell NPs. The fabrication processes can also be briefly divided into two steps: (1) electroless Ag plating on the Au NPs and (2) annealing of Au-Ag core-shell NPs. The first step deposits silver on the surface of Au NPs by electroless Ag plating method. The second step grows the uniform morphology of Au-Ag core-shell NPs by annealing the substrates at 400 °C for 1 h in a N_2 atmosphere.

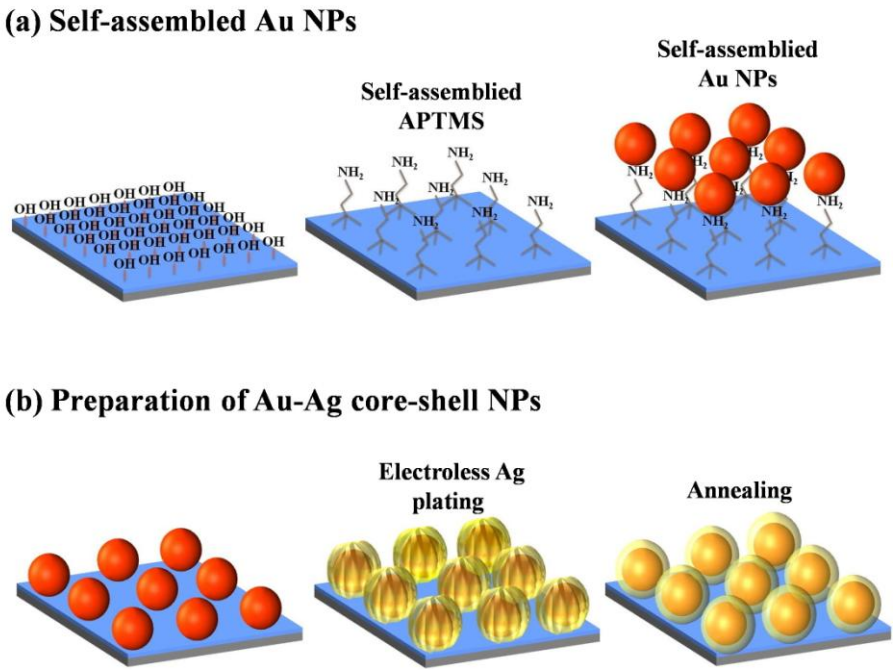

Figure 1. The two procedures used to fabricate Au-Ag core-shell NPs on the silicon substrate a) self-assembly Au NPs and b) preparation of Au-Ag core-shell NPs.

Figure 2a shows a top-view SEM image of Au NPs self-assembled on the Si substrate. After a deposition period of 10 min, the diameters and densities of Au NPs are 11.0 ± 1.9 nm and $2.9x10^3$ per micron^{-2}, respectively. The different sizes of Au-Ag core-shell NPs can be synthesized by electroless Ag plating at the different volumes of silver nitrate. Figure 2b-d show top-view SEM images of the different sizes of Au-Ag core-shell NPs deposited on the Si substrate and the volumes of silver nitrate are 3, 6 and 9 mL, respectively. The average diameters and densities of Au-Ag core-shell NPs are 16.1±4.2 nm ($1.3x10^3$ per micron^{-2}), 23.5±7.0 nm ($9.7x10^2$ per micron^{-2}) and 34.3±8.5 nm ($4.8x10^2$ per micron^{-2}), respectively. The sizes of Au-Ag core-shell NPs were significantly increasing with the increase in volumes of silver nitrate. On the other hand, the shell thicknesses of Au-Ag core-shell NPs can be effectively controlled by the volumes of silver nitrate. The densities of Au-Ag core-shell NPs are progressively decreasing with the increase in volumes of silver nitrate. The reverse tendency is ascribed to the neighboring Au-Ag core-shell NPs start to aggregate, form larger clumps and reducing the density after annealing at 400 °C for 1hr. This can be attributed to the coarsening of the Au and Ag structure driven by minimizing the total surface energy [27].

In our previous work, the quantity of Au NPs varies greatly, and increases with increasing holding time of spin coater [25, 26]. These results confirm that the holding time of spin coating for Au NPs plays a crucial role in determining the densities of Au NPs on the surface of the silicon substrate. The different densities of Au NPs are treated with so-called activators to form a catalytically active surface for subsequent electroless Ag plating. The densities of Au NPs and Au-Ag core-shell NPs (6 mL silver nitrate) was indeed found to significantly increase with the holding time of spin coating processes, as shown in Figure 3. The densities of Au NPs and Au-Ag core-shell NPs are 242(229), 1401(572) and 2925(775) per micron^{-2}, respectively.

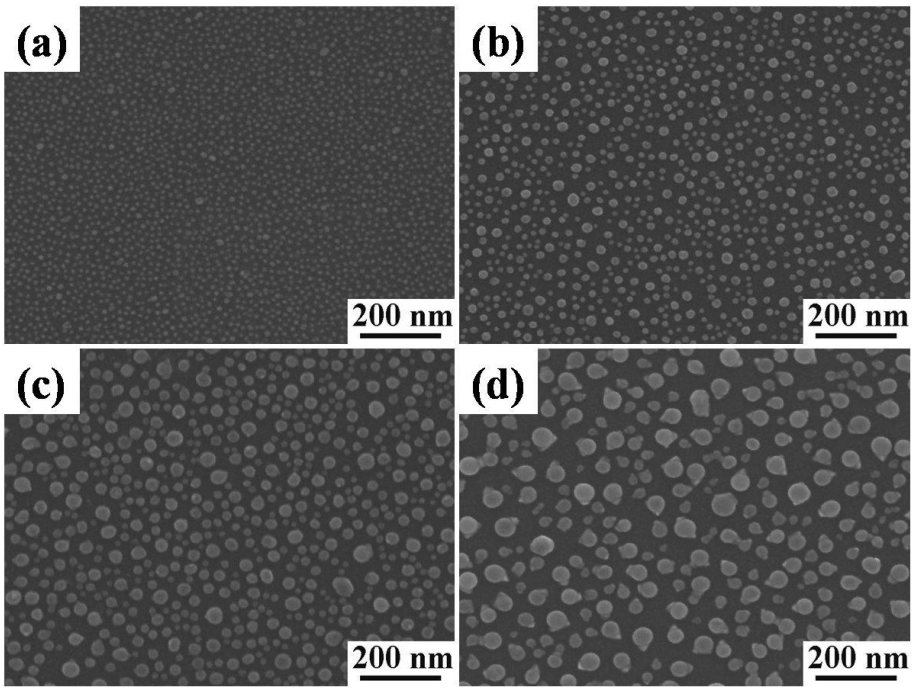

Figure 2. Top-view SEM images of a) Au NPs and b) Au-Ag core-shell NPs with the different volumes of silver nitrate were deposited on the silicon substrate.

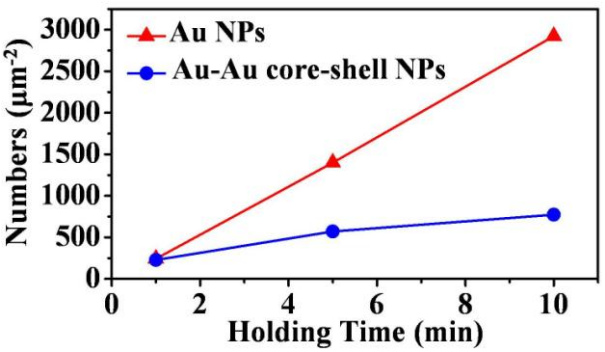

Figure 3. Curve of the holding time of spin coating processes versus the densities of the Au NPs and Au-Ag core-shell NPs.

The results indicate that spin-coating is an easy method for the density controllable self-assembly of Au NPs and the subsequent catalytic growth of Au-Ag core-shell NPs on a silicon substrate. The spin-coating strategy and electroless Ag plating in this study make it possible to grow the different densities and shell thicknesses of Au-Ag core-shell NPs.

The optical properties of Au NPs and Au-Ag core-shell NPs with different volumes of silver nitrate measured by UV-vis spectroscopy are depicted in Figure 4a. The UV-vis spectra of Au NPs and Au-Ag core-shell NPs appear the sharp and narrow peak with the maximum absorbance peak at the 519, 493, 486 and 480 nm, respectively. The absorption was caused by the surface Plasmon resonance (SPR) of the NPs.

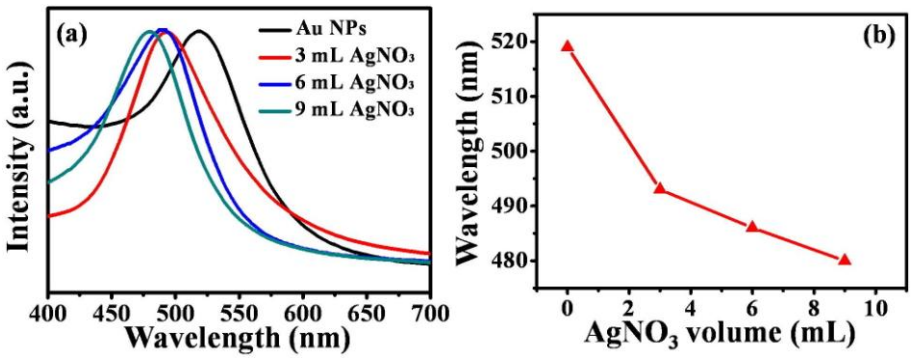

Figure 4. a) UV-vis spectra and b) the wavelength of maximum absorbance as a function of the volumes of silver nitrate.

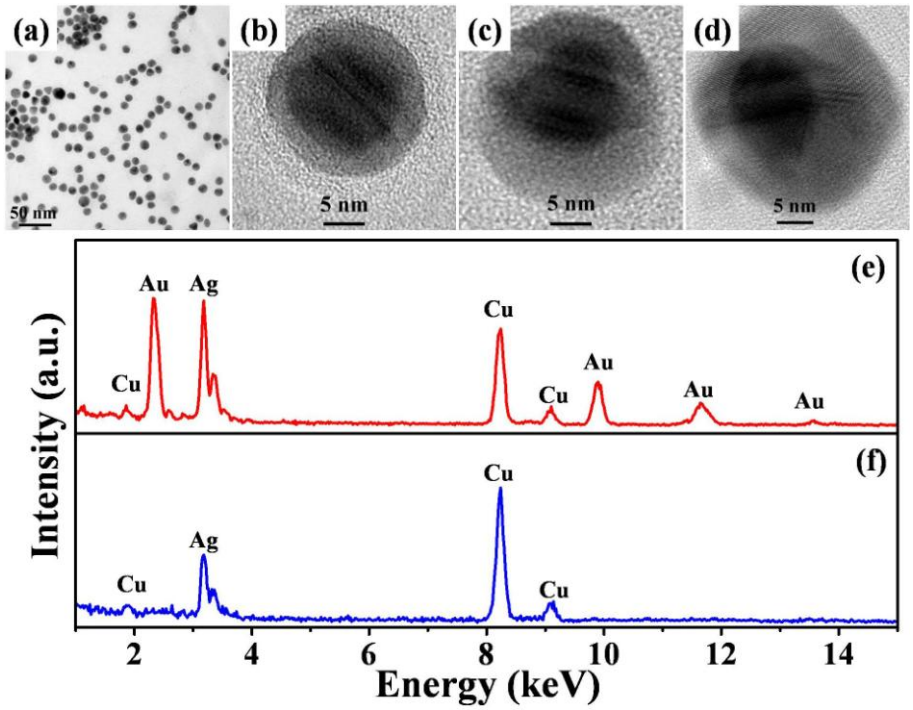

Figure 5. TEM images of a) Au NPs and b-d) an Au-Ag core-shell NP grown with 3, 6 and 9 mL silver nitrate solution, respectively. The EDS spectra of the e) center and f) side of Au-Ag core-shell NP.

As the metal of shell layer forms a thin uniform film on the core NPs, the SPR extinction band shows only one peak which results from the metal of shell layer [28]. The phenomenon of UV-vis spectra confirm that the formation of Au-Ag core-shell NPs is achieved by electroless Ag plating and annealing processes. The wavelength of maximum absorbance was significantly decreased with the increase in volumes of silver nitrate, as shown in Figure 4b. The blue shift of SPR band with increasing mole fraction of silver has been interpreted due to dampening of core. The dependence of nonlinear optical response of spherical core-shell NPs has been investigated as a function of relative composition of each metal [29]. Appropriate volumes of silver nitrate led to the growth of Au-Ag core-shell NPs with uniform sizes and varied shell thicknesses.

The morphology of the resultant Au NPs and Au-Ag core-shell NPs was determined by transmission electron microcopy (TEM). Figure 5a shows a low magnification TEM image of Au NPs. The average diameters of Au NPs are 10.8 ±1.7 nm. The variation of volumes of silver nitrate was found to affect the shell thicknesses of Ag. Figure 5b-d show TEM images of an Au-Ag core-shell NP with spherical geometry and grown for 3, 6, 9 mL silver nitrate solution, respectively. The TEM images clearly show the NP with core-shell structure. The shell thicknesses and sizes of Au-Ag core-shell NPs are 2.8 (19.2), 5.3 (24.1) and 8.0 (29.3) nm, respectively. The chemical composition of the NPs was analyzed by energy-dispersive spectroscopy (EDS). The EDS spectrum (Fig. 5e) shows that the elements of Au and Ag are present in the center of core-shell NP (Cu and C are from the TEM grid). As shown in Fig. 5f, the EDS spectrum reveals the only one element of Ag in the side of core-shell NP. These results confirm that the constituents are Au core and Ag shell. The correlation between the varied volumes of silver nitrate and electroless Ag plating method can be exploited to control the shell thicknesses and sizes of Au-Ag core-shell NPs.

SERS effect is very sensitive to the roughness of metal surface [16]. Herein the different shell thicknesses and densities of Au-Ag core-shell NPs were used as substrate to examine the SERS effect. Rhodamine B was chosen as the probe molecule owing to its well-established vibrational features [30,31]. Figure 6 a-d show the SERS spectra of rhodamine B solution ($1x10^{-4}$ M) dispersed on the Au NPs and different shell thicknesses of Au-Ag core-shell NPs. The strong and medium-strong Raman bands at 1198, 1279, 1357, 1509 and 1646 $cm^{-1}$are observed on the nanostructure surface. The strong peaks at ca. 1279, 1357, 1509 and 1646 cm^{-1} are assigned to the stretching modes of aromatic C-C. The band at 1198 cm^{-1} is assigned to aromatic C-H bending [31]. An obvious trend shows that the intensity of the Raman signal at 1646 cm^{-1} increased gradually with increasing the shell thicknesses of Au-Ag core-shell NPs and the maximum SERS signals are at the shell thicknesses of 5.3 nm, as shown in Figure 7. The SERS enhancement factor (EF) of Au-Ag core-shell NPs with the shell thicknesses of 5.3 nm is about 22 times rather than Au NPs. Compared with the Au-Ag core-shell NPs with 8.0 nm shell thicknesses, the densities was diminished and the shell thicknesses became thicker. It appears that the densities and shell thicknesses of Au-Ag core-shell NPs are main factors affecting SERS enhancement activity. According to the theoretical and experimental studies, the largest SERS enhancement occurs at the junction between two metal NPs [32-34]. As the number densities of Au-Ag core-shell NPs increases, the distance between the NPs decreases, therefore the number of junction increases providing a larger SERS enhancement. For the Au-Ag core shell NPs with 2.8 nm shell thicknesses, the shell thicknesses effects are expected to be relatively important. The 5.3 nm shell

thicknesses of Au-Ag core-shell NPs with the best SERS enhancement were fabricated by electroless Ag plating and annealing processes at the 6 mL silver nitrate.

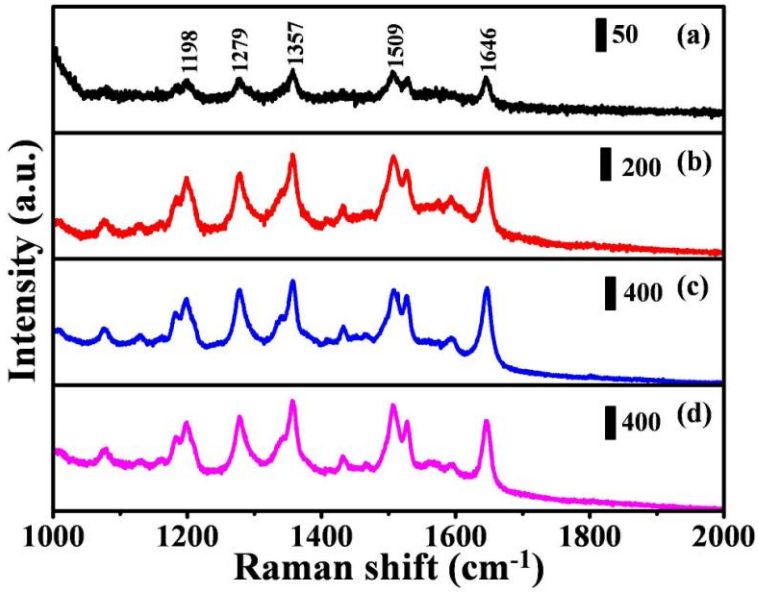

Figure 6. SERS spectra of rhodamine B ($1x10^{-4}$ M) absorbed on the silicon substrate with deposited a) Au NPs and different shell thicknesses of Au-Ag core-shell NPs. (b) 2.8, (c) 5.3 and (d) 8.0 nm.

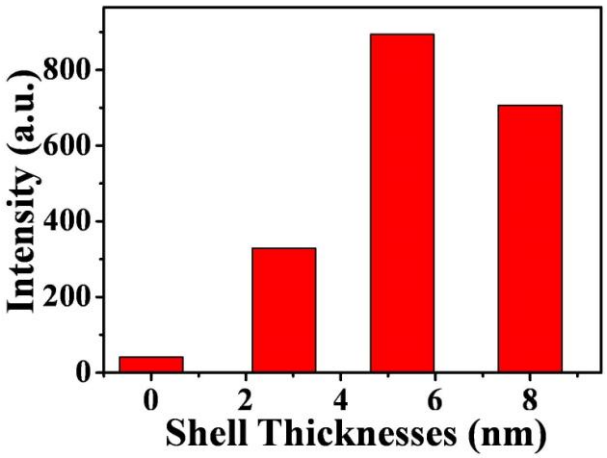

Figure 7. The maximum SERS intensity at 1646 cm^{-1} versus the Ag shell thicknesses.

Herein, the densities of Au-Ag core-shell NPs can also be controlled by varying the densities of Au NPs. The holding time of spin-coating processes is a facile method for the density controllable self-assembly of Au NPs. The Au NPs can be used to catalytic growth the different densities of Au-Ag core-shell NPs by electroless Ag plating processes on a silicon substrate. Figure 8 a-c show the Raman spectra of rhodamine B ($1x10^{-6}$ M) absorbed on the silicon substrate with the different densities of Au-Ag core-shell NP. The holding time of Au NPs are 1, 5 and 10 min, respectively. The densities of Au

NPs and Au-Ag core-shell NPs are the same with Figure 3. It appears that the densities of Au-Ag core-shell NPs are affecting SERS enhancement activity. The maximum SERS signals at 1646 cm^{-1} as a function of the densities is shown in Figure 9. The Au-Ag core-shell NPs have the maximum SERS signals at the Au NPs with holding time of 10 min. The appropriate densities of Au-Ag core-shell NPs were optimized to yield the greatest SERS effect in rhodamine B molecule. We believe that not only the high SERS activity of this substrate contributes to the high detection sensitivity, but also the sorption effect of the thick of Ag shell helps to improve the detection sensitivity

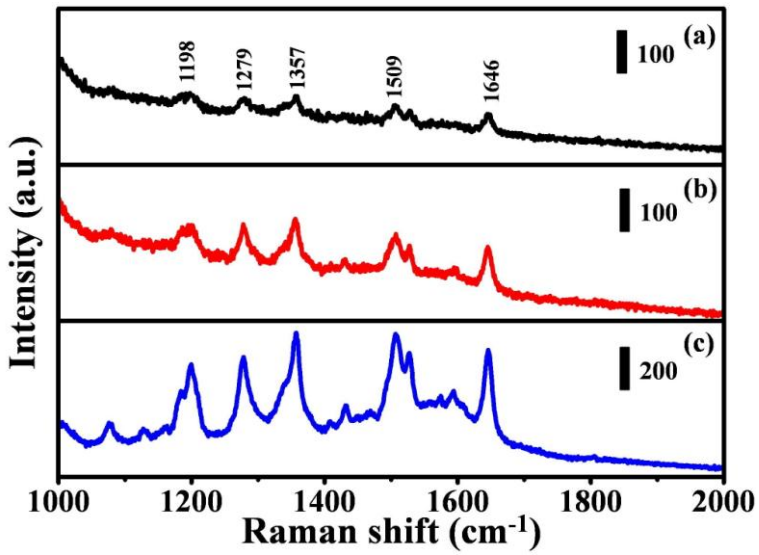

Figure 8. SERS spectra of rhodamine B ($1x10^{-6}$ M) absorbed Au-Ag core-shell NPs by electroless Ag plating (6 mL silver nitrate) on the silicon substrate with different holding time of Au NPs.

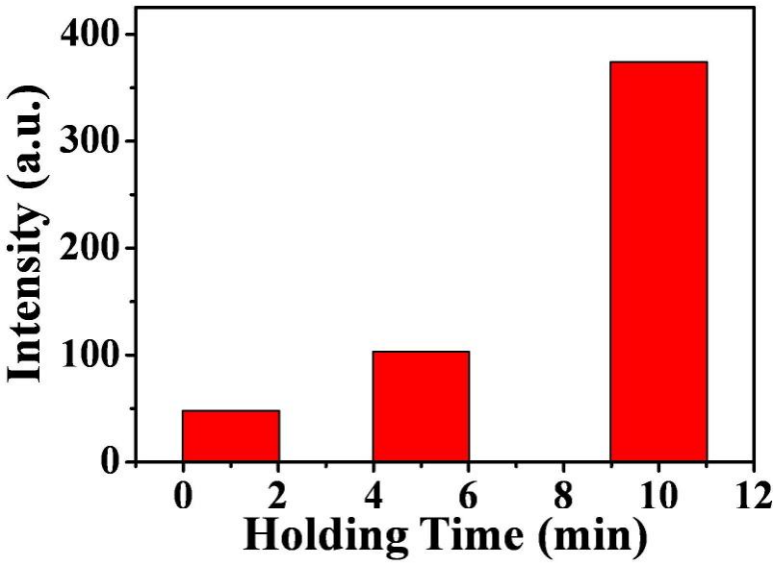

Figure 9. The maximum SERS intensity at 1646 cm^{-1} versus the holding time of Au NPs.

4. CONCLUSION

In summary, the uniform sizes of Au-Ag core-shell NPs with the different shell thicknesses can be synthesized by electroless Ag plating and annealing processes. The volumes of silver nitrate were found to be critical to control the shell thicknesses of Au-Ag core-shell NPs. The holding time of spin coating processes was important for growing the different densities of Au-Ag core-shell NPs on an APTMS-modified silicon substrate. The appropriate shell thicknesses and densities of Au-Ag core-shell NPs are beneficial to yield the greatest SERS effect of rhodamine B molecule. The combination spin-coating strategy and electroless plating method provide a facile, high enhancement and low cost fabrication, which shall be of significant value for practical applications of biosensor systems.

ACKNOWLEDGMENTS
This study was supported financially by the National Science Council, Taiwan (NSC 101-2811-M-390-001 and NSC 100-2113-M-390-002-MY3).

References

1. A. Wang, Y. P. Hsieh, Y. F. Chen, C. Y. Mou, *J. Catal*. 237 (2006) 197.
2. B. Rodríguez-González, A. Burrows, M. Watanabe, C. J. Kiely, L. M. L. Marzán, *J. Mater. Chem*. 15 (2005) 1755.
3. I-Im S. Lim, P. N. Njoki, H. Y. Park, X. Wang, L. Wang, D. Mott, C. J. Zhong, *Nanotechnology* 19 (2008) 305102.
4. S. Pande, S. K. Ghosh, S. Praharaj, S. Panigrahi, S. Basu, S. Jana, A. Pal, T. Tsukuda, T. Pal, *J. Phys. Chem.* C 111 (2007) 10806.
5. D. I. Gittins, A. S. Susha, R. Wannemacher, *Adv. Mater*. 14 (2002) 508.
6. F. Caruso, M. Spasova, V. Salgueirno-Maceria, *Adv. Mater*.13 (2001) 1090.
7. T. Pham, J. B. Jackson, N. J. Halas, T. R. Lee, *Langmuir* 18 (2002) 4915.
8. S. J. Oldenburg, J. B. Jackson, S. L. Westcott, N. J. Halas, *Appl. Phys. Lett*. 75 (1999) 2897.
9. Y. Kobayashi. V. Salgueirin˜o-Maceira, L. M. Liz-Marza´n, *Chem. Mater*.13 (2001) 1630.
10. M. Giersig, P. Mulvancy, *Langmuir* 12 (1996) 4329.
11. A. Dokoutchaev, J. T. James, S. C. Koene, S. Pathak, G. K. S. Prakash, M. E. Thompson, *Chem. Mater*. 11 (1999) 2389.
12. Y. Xia, N. Venkateswaran, D. Qin, J. Tien, G. M. Whitesides, *Langmuir* 14 (1998) 363.
13. K. M. Kulinowski, P. Jiang, H. Vaswani, V. L. Colvin, *Adv. Mater.* 12 (2000) 833.
14. C. H. Hsu, M. C. Yeh, K. L. Lo, L. J. Chen, *Langmuir* 23 (2007) 12111.
15. Y. Ma, W. Li, E. C. Cho, Z. Li, T. Yu, J. Zeng, Z. Xie, Y. Xia, *ACS Nano* 4 (2010) 6725.
16. M. E. Stewart, C. R. Anderton, L. B. Thompson, J. Maria, S. K. Gray, J. A. Rogers, R. G. Nuzzo, *Chem. Rev.* 108 (2008) 494.
17. M. Fan, G. F.S. Andrade, A. G. Brolo, *Anal. Chim. Acta* 693 (2011) 7.
18. B. Sharma, R. R. Frontiera, A. I. Henry, E. Ringe, R. P. V. Duyne, *Mater. Today* 15 (2012) 16.
19. M. Rycenga, C. M. Cobley, J. Zeng, W. Li, C. H. Moran, Q. Zhang, D. Qin, Y. Xia, *Chem. Rev.* 111 (2011) 3669.
20. I. Yoon, T. Kang, W. Choi, J. Kim, Y. Yoo, S. W. Joo, Q. H. Park, H. Ihee, B. Kim, *J. Am. Chem. Soc*. 131 (2009) 758.
21. A. Steinbrück, O. Stranik, A. Csaki, W. Fritzsche, *Anal. Bioanal. Chem*. 401 (2011) 1241.
22. M. Moskovits, I. Srnova´-Sÿ loufova´, B. Vlc˘kova´, *J. Chem. Phys*. 116 (2002) 10435.

23. R. G. Freeman, M. B. Hommer, K. C. Grabar, M. A. Jackson, M. J. Natan, *J. Phys. Chem*. 100 (1996) 718.
24. L. Rivas, S. Sanchez-Cortes, J. V. Garcı´a-Ramos, G. Morcillo, *Langmuir* 16 (2000) 9722.
25. F. K. Liu, P. W. Huang, Y. C. Chang, F. H. Ko, T. C. Chu, *Langmuir* 21 (2005) 2519.
26. T. H. Chang, Y. C. Lai, Y. C. Chang, F. H. Ko, F. K. Liu, *Int. J. Electrochem. Sci*. 7 (2012) 8140.
27. P. Y. Su, J. C. Hu, S. L. Cheng, L. J. Chen, J. M. Liang, *Appl. Phys. Lett*. 84 (2004) 3480.
28. S. Pande, S. K. Ghosh, S. Paharaj, S. Panigrahi, S. Basu, S. Jana, A. Pal, T. Tsukada, T. Pal, *J. Phys. Chem.* C 111 (2007) 10806.
29. S. Pyne, P. Sarkar, S. Basu, G. P. Sahoo, D. K. Bhui, H. Bar, A. Misra, *J. Nanopart. Res*. 13 (2011) 1759.
30. M. Volny, A. Sengupta, C. B. Wilson, B. D. Swanson, E. J. Davis, F. Turecek, *Anal. Chem.* 79 (2007) 4543.
31. M. T. Zin, K. Leong, N. Y. Wong, H. Ma, A. K. Y. Jen, *Nanotechnology*18 (2007) 455301.
32. V. A. Markel, V. M. Shalaev, P. Zhang, W. Huynh, L. Tay, T. L. Haslett, M. Moskovits, *Phys. Rev.* B 59 (1999) 10903.
33. Y. Wang, H. Chen, S. Dong, E. Wang, *J. Raman Spectrosc*. 38 (2007) 515.
34. C. Caro, C. Lopez-Cartes, J. A. Mejias, *J. Raman Spectrosc*. 39 (2008) 1162.